

# Intelligent Reflecting Surface Enabled Sensing: Cramér-Rao Lower Bound Optimization

Xianxin Song\*, Jie Xu\*, Fan Liu†, Tony Xiao Han‡, and Yonina C. Eldar§

\*School of Science and Engineering, Future Network of Intelligence Institute, and Guangdong Provincial Key Laboratory of Future Networks of Intelligence, The Chinese University of Hong Kong (Shenzhen), China

†Department of Electrical and Electronic Engineering, Southern University of Science and Technology, China

‡Wireless Technology Lab, 2012 Laboratories, Huawei, China

§Faculty of Mathematics and Computer Science, Weizmann Institute of Science, Israel

Email: xianxinsong@link.cuhk.edu.cn, xujie@cuhk.edu.cn, liuf6@sustech.edu.cn,

tony.hanxiao@huawei.com, yonina.eldar@weizmann.ac.il

**Abstract**—This paper investigates intelligent reflecting surface (IRS) enabled non-line-of-sight (NLoS) wireless sensing, in which an IRS is dedicatedly deployed to assist an access point (AP) to sense a target at its NLoS region. It is assumed that the AP is equipped with multiple antennas and the IRS is equipped with a uniform linear array. The AP aims to estimate the target’s direction-of-arrival (DoA) with respect to the IRS based on the echo signal from the AP-IRS-target-IRS-AP link. Under this setup, we jointly design the transmit beamforming at the AP and the reflective beamforming at the IRS to minimize the DoA estimation error in terms of Cramér-Rao lower bound (CRLB). Towards this end, we first obtain the closed-form expression of CRLB for DoA estimation. Next, we optimize the joint beamforming design to minimize the obtained CRLB, via alternating optimization, semi-definite relaxation, and successive convex approximation. Finally, numerical results show that the proposed design based on CRLB minimization achieves improved sensing performance in terms of lower estimation mean squared error (MSE), as compared to the traditional schemes with signal-to-noise ratio maximization and separate beamforming designs.

## I. INTRODUCTION

Integrating wireless (radar) sensing into future beyond-fifth-generation (B5G) and six-generation (6G) wireless networks as a new functionality has attracted growing research interest to support various environment-aware applications such as industrial automation, auto-driving, and remote healthcare (see, e.g., [1]–[3] and the references therein). Conventionally, wireless sensing relies on line-of-sight (LoS) links between the access points (APs) (or sensing transceivers) and the sensing targets, such that the sensing information (e.g., the distance/velocity/angle of targets) can be extracted based on the target echo signals. However, in practical scenarios with dense obstructions, the sensing targets are highly likely to be located at the non-LoS (NLoS) region of APs, where conventional LoS sensing is not applicable in general. Therefore, how to realize NLoS sensing in such scenarios is a challenging task.

Motivated by its success in wireless communications [4]–[6], intelligent reflecting surface (IRS) or reconfigurable intelligent surface (RIS) have become a viable new solution

to overcome this issue (see, e.g., [1], [7]–[11]). By properly deploying IRSs around the AP to reconfigure the radio propagation environment, virtual LoS links can be established between the AP and the targets in its NLoS region, such that the AP can perform the NLoS target sensing based on the echo signals from AP-IRS-target-IRS-AP links. To combat the severe signal propagation loss over such triple-reflected links, the IRS can adaptively control the phases at reflecting elements, such that the reflected signals are beamed towards desired target directions to enhance sensing performance.

There have been several prior works investigating IRS-enabled wireless sensing [7]–[10] and IRS-enabled integrated sensing and communications (ISAC) [1], [11], respectively. For instance, the work [7] presented the NLoS radar equation based on the AP-IRS-target-IRS-AP link and evaluated the resultant sensing performance in terms of signal-to-noise ratio (SNR) and signal-to-clutter ratio (SCR). In [8], the authors considered an IRS-enabled bi-static target estimation, where dedicated sensors were installed at the IRS for estimating the direction of its nearby target through the AP-IRS-target-sensors link. Under this setup, the authors optimized the IRS’s reflective beamforming to maximize the average received signal power at the sensors and applied the multiple signal classification (MUSIC) algorithm for estimating targets. In [9] and [10], the authors considered IRS-enabled target detection, in which the IRS’s passive beamforming was optimized to maximize the target detection probability subject to a fixed false alarm probability. In [1], the authors considered an IRS-enabled ISAC system with one base station (BS), one communication user (CU), and multiple targets, in which the IRS’s minimum beampattern gain towards the desired sensing angles was maximized by jointly optimizing the transmit beamforming at the IRS and the reflective beamforming at the IRS, subject to the minimum SNR requirement at the CU. In [11], the authors considered an IRS-enabled ISAC system with one BS, one CU, and one target, in which the SNR of radar was maximized by joint beamforming design while ensuring the SNR at the CU.

In most prior works on IRS-enabled sensing and IRS-enabled ISAC, the sensing SNR and target detection probability were adopted as the sensing performance metrics for

optimization. To our best knowledge, how to analyze the performance for NLoS target estimation through AP-IRS-target-IRS-AP links and optimize such performance by joint transmit and reflective beamforming design are still uncharted areas. This thus motivates this work to analyze and optimize the target estimation error performance of IRS-enabled sensing, by particularly considering the estimation Cramér-Rao lower bound (CRLB) as the performance metric. In general, CRLB provides a lower bound on the variance of unbiased parameter estimators and has been widely adopted as a metric for evaluating the estimation performance in wireless sensing systems without IRS [12]–[14].

This paper considers an IRS-enabled NLoS wireless sensing system, which consists of one AP with multiple antennas, one IRS with a uniform linear array (ULA), and one target at the NLoS region of the AP. The AP aims to estimate the target's direction-of-arrival (DoA) with respect to (w.r.t.) the IRS based on the echo signal from the AP-IRS-target-IRS-AP link. In particular, we focus on the narrowband transmission for IRS-enabled sensing, in which a general multi-path channel model (including both LoS and NLoS paths) is considered for the AP-IRS link, and an LoS channel model is considered for the IRS-target link to facilitate DoA estimation. It is assumed that the AP perfectly knows the channel state information (CSI) of the AP-IRS link, and needs to estimate the target's DoA and the channel coefficient of the IRS-target-IRS link as unknown parameters. Under this setup, we aim to minimize the DoA estimation error in terms of the estimation CRLB, by jointly optimizing the transmit beamforming at the AP and the reflective beamforming at the IRS. Towards this end, we first obtain the CRLB for DoA estimation in closed form. Based on the obtained CRLB, it is shown that the target's DoA is only estimable when the rank of the AP-IRS channel matrix is higher than one or equivalently there are more than one signal paths in that channel. Next, we minimize the obtained CRLB by jointly optimizing the transmit and reflective beamforming, subject to a maximum power constraint at the AP.

Although the formulated CRLB minimization problem is non-convex and difficult to solve, we present an efficient algorithm to obtain a high-quality solution via alternating optimization, semi-definite relaxation (SDR), and successive convex approximation (SCA). Then, we present the maximum likelihood estimation (MLE) to estimate the target's DoA, for which the achieved estimation mean squared error (MSE) is shown to coverage towards the CRLB when the SNR becomes sufficiently high. Finally, numerical results show that the proposed joint beamforming design based on CRLB minimization achieves improved sensing performance in terms of estimation MSE, as compared to the traditional schemes with SNR maximization and separate beamforming designs.

*Notations:* Boldface letters refer to vectors (lower case) or matrices (upper case). For a square matrix  $\mathbf{S}$ ,  $\text{tr}(\mathbf{S})$  and  $\mathbf{S}^{-1}$  denote its trace and inverse, respectively, and  $\mathbf{S} \succeq \mathbf{0}$  means that  $\mathbf{S}$  is positive semi-definite. For an arbitrary-size matrix  $\mathbf{M}$ ,  $\text{rank}(\mathbf{M})$ ,  $\mathbf{M}^*$ ,  $\mathbf{M}^T$ , and  $\mathbf{M}^H$  are its rank, conjugate transpose, and conjugate transpose, respectively. The matrix  $\mathbf{I}_m$  is an identity matrix of dimension  $m$ . We use  $\mathcal{CN}(\mathbf{x}, \Sigma)$  to denote the distribution of a circularly symmetric complex

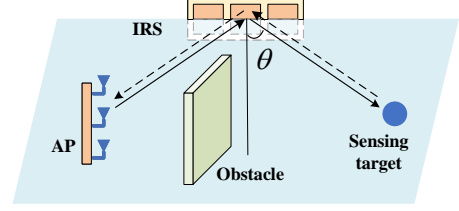


Figure 1. System model of IRS-enabled sensing.

Gaussian (CSCG) random vector with mean vector  $\mathbf{x}$  and covariance matrix  $\Sigma$ , and  $\sim$  to denote “distributed as”. The spaces of  $x \times y$  complex and real matrices are denoted by  $\mathbb{C}^{x \times y}$  and  $\mathbb{R}^{x \times y}$ , respectively. The real and imaginary parts of a complex number are denoted by  $\text{Re}\{\cdot\}$  and  $\text{Im}\{\cdot\}$ , respectively. The symbol  $\mathbb{E}(\cdot)$  denotes the statistical expectation,  $\|\cdot\|$  stands for the Euclidean norm,  $|\cdot|$  for the magnitude of a complex number,  $\text{diag}(a_1, \dots, a_N)$  for a diagonal matrix with diagonal elements  $a_1, \dots, a_N$ ,  $\otimes$  for the Kronecker product,  $\text{vec}(\cdot)$  for the vectorization operator, and  $\arg(\mathbf{x})$  for a vector with each element being the phase of the corresponding element in  $\mathbf{x}$ .

## II. SYSTEM MODEL

We consider an IRS-enabled NLoS wireless sensing system as shown in Fig. 1, which consists of one AP with  $M > 1$  antennas, one ULA-IRS with  $N > 1$  reflecting elements, and one target at the NLoS region of the AP (i.e., the LoS link between the AP and the target is blocked by obstacles such as buildings and trees). The IRS is deployed to create a virtual LoS link to facilitate the target sensing. In this case, the AP transmits sensing signal and then estimates the target's DoA w.r.t. the IRS based on the echo signal from the AP-IRS-target-IRS-AP link. Note that the target estimation should be implemented at the AP instead of the IRS, as the IRS is normally a passive device without the capability of signal processing.

First, we consider the transmit and reflective beamforming at the AP and the IRS, respectively. Let  $\mathbf{x}(t)$  denote the transmitted signal by the AP at time slot  $t$  and  $T$  the radar dwell time. The sample coherence matrix of the transmitted signal is

$$\mathbf{R}_x = \frac{1}{T} \sum_{t=1}^T \mathbf{x}(t) \mathbf{x}(t)^H,$$

which corresponds to the transmit beamforming vectors to be optimized. Suppose that  $\text{rank}(\mathbf{R}_x) = k$  and the eigenvalue decomposition (EVD) of  $\mathbf{R}_x$  is given by  $\mathbf{R}_x = \mathbf{W} \mathbf{\Lambda} \mathbf{W}^H$ , where  $\mathbf{\Lambda} = \text{diag}(\lambda_1, \dots, \lambda_M)$  and  $\mathbf{W} = [\mathbf{w}_1, \dots, \mathbf{w}_M]$  with  $\lambda_1 \geq \dots \geq \lambda_k > \lambda_{k+1} = \dots = \lambda_M = 0$ , and  $\mathbf{W} \mathbf{W}^H = \mathbf{W}^H \mathbf{W} = \mathbf{I}_M$ . This means that there are a number of  $k$  sensing beams transmitted by the AP, each of which is denoted by  $\sqrt{\lambda_i} \mathbf{w}_i, i = 1, \dots, k$  (see, e.g., [15]). As for the reflective beamforming, we consider that the IRS can only adjust the phase shifts of its reflecting elements [4]. Let  $\mathbf{v} = [e^{j\phi_1}, \dots, e^{j\phi_N}]^T$  denote the reflective beamforming vector at the IRS, with  $\phi_n \in (0, 2\pi]$  being the phase shift of element  $n \in \{1, \dots, N\}$  at the IRS, which can be optimized later to enhance the sensing performance.

Next, we introduce the channel model. We consider a general multi-path model for the AP-IRS link. Accordingly, let  $\mathbf{G} \in \mathbb{C}^{N \times M}$  denote the associated channel matrix of the AP-IRS link, where  $\text{rank}(\mathbf{G}) \geq 1$  holds in general. We consider an LoS model for the IRS-target link to facilitate DoA estimation. Let  $\theta$  denote the target's DoA w.r.t. the IRS. Accordingly, the steering vector at the IRS with angle  $\theta$  is

$$\mathbf{a}(\theta) = [1, e^{j2\pi \frac{d_{\text{IRS}} \sin \theta}{\lambda}}, \dots, e^{j2\pi \frac{(N-1)d_{\text{IRS}} \sin \theta}{\lambda}}]^T, \quad (1)$$

where  $d_{\text{IRS}}$  denotes the spacing between consecutive reflecting elements at the IRS and  $\lambda$  denotes the carrier wavelength. The target response matrix w.r.t. the IRS (or equivalently the cascaded IRS-target-IRS channel) is

$$\mathbf{H} = \alpha \mathbf{a}(\theta) \mathbf{a}^T(\theta),$$

where  $\alpha \in \mathbb{C}$  denotes the complex-valued channel coefficient dependent on the target's radar cross section (RCS) and the round-trip path loss of the IRS-target-IRS link. Note that the target's DoA  $\theta$  and the channel coefficient  $\alpha$  are both unknown parameters to be estimated by the AP.

Based on the transmitted signal  $\mathbf{x}(t)$  and channel models, the signal impinged at the IRS is  $\mathbf{G}\mathbf{x}(t)$ . After the reflective beamforming at the IRS and target reflection, the echo signal impinged at the IRS becomes  $\mathbf{H}\Phi\mathbf{G}\mathbf{x}(t)$ , where  $\Phi = \text{diag}(\mathbf{v})$  denotes the reflection matrix of the IRS. By further reflective beamforming at IRS and through the IRS-AP channel, the received echo signal at the AP through the whole AP-IRS-target-IRS-AP link at time  $t \in \{1, \dots, T\}$  is

$$\begin{aligned} \mathbf{y}(t) &= \mathbf{G}^T \Phi^T \mathbf{H} \Phi \mathbf{G} \mathbf{x}(t) + \mathbf{n}(t) \\ &= \alpha \mathbf{G}^T \Phi^T \mathbf{a}(\theta) \mathbf{a}^T(\theta) \Phi \mathbf{G} \mathbf{x}(t) + \mathbf{n}(t), \end{aligned} \quad (2)$$

where  $\mathbf{n}(t) \sim \mathcal{CN}(\mathbf{0}, \sigma^2 \mathbf{I}_M)$  denotes the additive white Gaussian noise (AWGN) at the AP receiver.

The AP aims to estimate the unknown parameters (including the target's DoA  $\theta$  and the channel coefficient  $\alpha$ ), based on the received echo signal in (2). It is assumed that the AP perfectly knows the CSI  $\mathbf{G}$  of the AP-IRS link via proper channel estimation algorithms (see, e.g., [16]). This assumption is practically valid, which is due to the fact that the AP and the IRS are deployed at fixed locations and thus their channels are slowly varying in practice. It is also assumed that the AP perfectly knows its transmitted signal  $\mathbf{x}(t)$  (and the associated coherence matrix  $\mathbf{R}_x$ ) and the IRS's reflective beamforming vector  $\mathbf{v}$ , which can be optimized to enhance the sensing performance. In the following, we first obtain the CRLB for DoA estimation from  $\mathbf{y}(t)$  in Section III, and then minimize the obtained CRLB via jointly optimizing the transmit beamforming  $\mathbf{R}_x$  and the reflective beamforming  $\mathbf{v}$  in Section IV.

### III. ESTIMATION CRLB DERIVATION

This section analyzes the estimation performance in the IRS-enabled NLoS wireless sensing system, in terms of CRLB. Let  $\boldsymbol{\xi} = [\theta, \tilde{\alpha}^T]^T$  denote the vector of unknown parameters to be estimated, including the target's DoA  $\theta$  and the complex-valued channel coefficient  $\alpha$ , where  $\tilde{\alpha} =$

$[\text{Re}\{\alpha\}, \text{Im}\{\alpha\}]^T$ . We are particularly interested in characterizing the CRLB for estimating the target's DoA  $\theta$ . This is due to the fact that it is difficult to extract the target information from the channel coefficient  $\alpha$ , as it depends on both the target's RCS and the distance-dependent path loss of the IRS-target-IRS link that are usually unknown.

First, we obtain the Fisher information matrix (FIM) for estimating  $\boldsymbol{\xi}$  to facilitate the derivation of the CRLB for DoA estimation. Towards this end, we stack the transmitted signals, the received signals, and the noise over the radar dwell time as  $\mathbf{X} = [\mathbf{x}(1), \dots, \mathbf{x}(T)]$ ,  $\mathbf{Y} = [\mathbf{y}(1), \dots, \mathbf{y}(T)]$ , and  $\mathbf{N} = [\mathbf{n}(1), \dots, \mathbf{n}(T)]$ , respectively. Accordingly, we have

$$\mathbf{Y} = \alpha \mathbf{B}(\theta) \mathbf{X} + \mathbf{N}, \quad (3)$$

where  $\mathbf{B}(\theta) = \mathbf{b}(\theta) \mathbf{b}(\theta)^T$  with  $\mathbf{b}(\theta) = \mathbf{G}^T \Phi^T \mathbf{a}(\theta)$ . For notational convenience, in the sequel we drop  $\theta$  in  $\mathbf{a}(\theta)$ ,  $\mathbf{b}(\theta)$ , and  $\mathbf{B}(\theta)$ , and accordingly denote them as  $\mathbf{a}$ ,  $\mathbf{b}$ , and  $\mathbf{B}$ , respectively. By vectorizing (3), we have

$$\tilde{\mathbf{y}} = \text{vec}(\mathbf{Y}) = \tilde{\mathbf{u}} + \tilde{\mathbf{n}}, \quad (4)$$

where  $\tilde{\mathbf{u}} = \alpha \text{vec}(\mathbf{B}\mathbf{X})$  and  $\tilde{\mathbf{n}} = \text{vec}(\mathbf{N}) \sim \mathcal{CN}(\mathbf{0}, \mathbf{R}_n)$  with  $\mathbf{R}_n = \sigma^2 \mathbf{I}_{MT}$ . Let  $\mathbf{F} \in \mathbb{R}^{3 \times 3}$  denote the FIM matrix for estimating  $\boldsymbol{\xi}$  based on (4). Since  $\tilde{\mathbf{n}}$  is AWGN, each element of  $\mathbf{F}$  is given by [12]

$$\begin{aligned} \mathbf{F}_{i,j} &= \text{tr} \left( \mathbf{R}_n^{-1} \frac{\partial \mathbf{R}_n}{\partial \xi_i} \mathbf{R}_n^{-1} \frac{\partial \mathbf{R}_n}{\partial \xi_j} \right) \\ &\quad + 2 \text{Re} \left\{ \frac{\partial \tilde{\mathbf{u}}^H}{\partial \xi_i} \mathbf{R}_n^{-1} \frac{\partial \tilde{\mathbf{u}}}{\partial \xi_j} \right\}, \quad i, j = 1, 2, 3. \end{aligned} \quad (5)$$

Based on (5), the FIM matrix  $\mathbf{F}$  can be partitioned as

$$\mathbf{F} = \begin{bmatrix} \mathbf{F}_{\theta\theta} & \mathbf{F}_{\theta\tilde{\alpha}} \\ \mathbf{F}_{\theta\tilde{\alpha}}^T & \mathbf{F}_{\tilde{\alpha}\tilde{\alpha}} \end{bmatrix}, \quad (6)$$

where

$$\mathbf{F}_{\theta\theta} = \frac{2T|\alpha|^2}{\sigma^2} \text{tr}(\dot{\mathbf{B}}\mathbf{R}_x \dot{\mathbf{B}}^H),$$

$$\mathbf{F}_{\theta\tilde{\alpha}} = \frac{2T}{\sigma^2} \text{Re}\{\alpha^* \text{tr}(\mathbf{B}\mathbf{R}_x \dot{\mathbf{B}}^H)[1, j]\},$$

$$\mathbf{F}_{\tilde{\alpha}\tilde{\alpha}} = \frac{2T}{\sigma^2} \text{tr}(\mathbf{B}\mathbf{R}_x \mathbf{B}^H) \mathbf{I}_2,$$

with  $j = \sqrt{-1}$  and  $\dot{\mathbf{B}} = \frac{\partial \mathbf{B}}{\partial \theta}$  denotes the partial derivative of  $\mathbf{B}$  w.r.t.  $\theta$ . Note that the derivation of the FIM  $\mathbf{F}$  follows the standard procedure in [13], for which the details can be referred to in Appendix A.

Next, we derive the CRLB for DoA estimation, which corresponds to the first diagonal element of  $\mathbf{F}^{-1}$ , i.e.,

$$\text{CRLB}(\theta) = [\mathbf{F}^{-1}]_{1,1} = [\mathbf{F}_{\theta\theta} - \mathbf{F}_{\theta\tilde{\alpha}} \mathbf{F}_{\tilde{\alpha}\tilde{\alpha}}^T \mathbf{F}_{\theta\tilde{\alpha}}]^{-1}. \quad (7)$$

Based on (7) and (6), we have the following lemma.

**Lemma 1.** The CRLB for DoA  $\theta$  estimation is given by

$$\text{CRLB}(\theta) = \frac{\sigma^2}{2T|\alpha|^2 \left( \text{tr}(\dot{\mathbf{B}}\mathbf{R}_x \dot{\mathbf{B}}^H) - \frac{|\text{tr}(\mathbf{B}\mathbf{R}_x \dot{\mathbf{B}}^H)|^2}{\text{tr}(\mathbf{B}\mathbf{R}_x \mathbf{B}^H)} \right)}. \quad (8)$$

To gain more insight and facilitate the reflective beamforming design, we re-express  $\text{CRLB}(\theta)$  in (8) w.r.t. the reflective beamforming vector  $\mathbf{v}$ . Towards this end, we introduce

$$\text{CRLB}(\theta) = \frac{\sigma^2}{2T|\alpha|^2\pi^2 \cos^2(\theta) \left( \mathbf{v}^H \mathbf{R}_2 \mathbf{v} \left( \mathbf{v}^H \mathbf{D} \mathbf{R}_1 \mathbf{D} \mathbf{v} - \frac{|\mathbf{v}^H \mathbf{D} \mathbf{R}_1 \mathbf{v}|^2}{\mathbf{v}^H \mathbf{R}_1 \mathbf{v}} \right) + \mathbf{v}^H \mathbf{R}_1 \mathbf{v} \left( \mathbf{v}^H \mathbf{D} \mathbf{R}_2 \mathbf{D} \mathbf{v} - \frac{|\mathbf{v}^H \mathbf{D} \mathbf{R}_2 \mathbf{v}|^2}{\mathbf{v}^H \mathbf{R}_2 \mathbf{v}} \right) \right)} \quad (11)$$

$\mathbf{A} = \text{diag}(\mathbf{a})$ , and accordingly have  $\mathbf{b} = \mathbf{G}^T \Phi^T \mathbf{a} = \mathbf{G}^T \mathbf{A} \mathbf{v}$ . Then, let  $\dot{\mathbf{b}}$  denote the partial derivative of  $\mathbf{b}$  w.r.t.  $\theta$ . We have  $\dot{\mathbf{b}} = j\pi \cos \theta \mathbf{G}^T \Phi^T \mathbf{D} \mathbf{a} = j\pi \cos \theta \mathbf{G}^T \mathbf{A} \mathbf{D} \mathbf{v}$  with  $\mathbf{D} = \text{diag}(0, 1, \dots, N-1)$ . As a result,

$$\mathbf{B} = \mathbf{b} \mathbf{b}^T = \mathbf{G}^T \mathbf{A} \mathbf{v} \mathbf{v}^T \mathbf{A}^T \mathbf{G}, \quad (9)$$

$$\begin{aligned} \dot{\mathbf{B}} &= \dot{\mathbf{b}} \mathbf{b}^T + \mathbf{b} \dot{\mathbf{b}}^T \\ &= j\pi \cos \theta \mathbf{G}^T \mathbf{A} (\mathbf{D} \mathbf{v} \mathbf{v}^T + \mathbf{v} \mathbf{v}^T \mathbf{D}^T) \mathbf{A}^T \mathbf{G}. \end{aligned} \quad (10)$$

Substituting (9) and (10) into (8), we re-express  $\text{CRLB}(\theta)$  w.r.t.  $\mathbf{v}$  in (11) at the top of this page, where  $\mathbf{R}_1 = \mathbf{A}^H \mathbf{G}^* \mathbf{G}^T \mathbf{A}$  and  $\mathbf{R}_2 = \mathbf{A}^H \mathbf{G}^* \mathbf{R}_x^* \mathbf{G}^T \mathbf{A}$ .

Based on  $\text{CRLB}(\theta)$  in (11), we have the following proposition.

**Proposition 1.** If  $\text{rank}(\mathbf{G}) = 1$  (or equivalently there is only one single path between the AP and the IRS), then the FIM  $\mathbf{F}$  in (5) for estimating  $\xi$  is a singular matrix, and  $\text{CRLB}(\theta) = \infty$ . Otherwise, the FIM  $\mathbf{F}$  is invertible, and  $\text{CRLB}(\theta)$  is bounded.

*Proof.* See Appendix B.

Proposition 1 shows that the target's DoA  $\theta$  is estimable only when  $\text{rank}(\mathbf{G}) > 1$  (i.e., the number of signal paths between the AP and the IRS is larger than one). The reasons are intuitively explained as follows. When  $\text{rank}(\mathbf{G}) = 1$ , the truncated singular value decomposition (SVD) of  $\mathbf{G}$  is expressed as  $\mathbf{G} = \sigma_1 \hat{\mathbf{u}}_1 \hat{\mathbf{v}}_1^T$ , where  $\hat{\mathbf{u}}_1$  and  $\hat{\mathbf{v}}_1$  are the left and right dominant singular vectors, and  $\sigma_1$  denotes the dominant singular value. Accordingly, the received echo signal in (2) at the AP is given by

$$\mathbf{y}(t) = \alpha \sigma_1^2 \hat{\mathbf{v}}_1 \underbrace{\hat{\mathbf{u}}_1^T \Phi^T \mathbf{a} \mathbf{a}^T \Phi \hat{\mathbf{u}}_1}_{\beta(\theta)} \underbrace{\hat{\mathbf{v}}_1^T \mathbf{x}(t)}_{\tilde{x}(t)} + \mathbf{n}(t), \quad (12)$$

where  $\beta(\theta) = |\hat{\mathbf{u}}_1^T \Phi^T \mathbf{a}|^2$  is the only scalar term related to  $\theta$ . Notice that in (12), the complex numbers  $\alpha$  and  $\beta(\theta)$  are coupled, and from  $\mathbf{y}(t)$  we can only recover one observation on  $\alpha\beta(\theta)$ , which is not sufficient to extract  $\beta(\theta)$ , thus making  $\theta$  not estimable.

#### IV. JOINT BEAMFORMING DESIGN FOR CRLB MINIMIZATION

In this section, we propose to jointly optimize the transmit beamforming at the AP and the reflective beamforming at the IRS to minimize the CRLB for DoA estimation in (8) or (11), subject to the maximum transmit power constraint at the AP. Note that in order to implement the joint beamforming design, we assume that the AP roughly knows the information of  $\theta$ , which is practically valid for a target tracking scenario. Also note that the channel coefficient  $\alpha$  is independent of the joint

beamforming design. Then the CRLB minimization problem is formulated as

$$(P1) : \min_{\mathbf{R}_x, \mathbf{v}} \text{CRLB}(\theta)$$

$$\text{s.t. } \text{tr}(\mathbf{R}_x) \leq P_0 \quad (13a)$$

$$\mathbf{R}_x \succeq \mathbf{0} \quad (13b)$$

$$\Phi = \text{diag}(\mathbf{v}) \quad (13c)$$

$$|\mathbf{v}_n| = 1, \forall n \in \{1, \dots, N\}, \quad (13d)$$

where  $P_0$  is the maximum transmit power budget at the AP. Note that problem (P1) is non-convex due to the non-concavity of the objective function and the unit-modulus constraint in (13d), which is thus difficult to be optimally solved.

To solve the non-convex problem (P1), we propose an efficient algorithm based on the principle of alternating optimization, in which the transmit beamformer  $\mathbf{R}_x$  at the AP and the reflective beamformer  $\mathbf{v}$  at the IRS are optimized in an alternating manner. In the following, we focus on optimizing  $\mathbf{R}_x$  and  $\mathbf{v}$ , respectively, with the other to be given.

##### A. Transmit Beamforming Optimization

First, we optimize the transmit beamformer  $\mathbf{R}_x$  in problem (P1) under any given reflective beamformer  $\mathbf{v}$ , in which the CRLB formula in (8) is used. In this case, minimizing  $\text{CRLB}(\theta)$  is equivalent to maximizing  $\text{tr}(\dot{\mathbf{B}} \mathbf{R}_x \dot{\mathbf{B}}^H) - \frac{|\text{tr}(\mathbf{B} \mathbf{R}_x \dot{\mathbf{B}}^H)|^2}{\text{tr}(\mathbf{B} \mathbf{R}_x \mathbf{B}^H)}$ . As a result, the transmit beamforming optimization problem is formulated as

$$(P2) : \max_{\mathbf{R}_x} \text{tr}(\dot{\mathbf{B}} \mathbf{R}_x \dot{\mathbf{B}}^H) - \frac{|\text{tr}(\mathbf{B} \mathbf{R}_x \dot{\mathbf{B}}^H)|^2}{\text{tr}(\mathbf{B} \mathbf{R}_x \mathbf{B}^H)}$$

s.t. (13a) and (13b).

By introducing an auxiliary variable  $t$ , problem (P2) is equivalently re-expressed as

$$(P2.1) : \max_{\mathbf{R}_x, t} t$$

s.t.  $\text{tr}(\dot{\mathbf{B}} \mathbf{R}_x \dot{\mathbf{B}}^H) - \frac{|\text{tr}(\mathbf{B} \mathbf{R}_x \dot{\mathbf{B}}^H)|^2}{\text{tr}(\mathbf{B} \mathbf{R}_x \mathbf{B}^H)} \geq t \quad (14a)$

(13a) and (13b).

Using the Schur complement [17], the constraint in (14a) is equivalently transformed into the following convex semi-definite constraint:

$$\begin{bmatrix} \text{tr}(\dot{\mathbf{B}} \mathbf{R}_x \dot{\mathbf{B}}^H) - t & \text{tr}(\mathbf{B} \mathbf{R}_x \dot{\mathbf{B}}^H) \\ \text{tr}(\dot{\mathbf{B}} \mathbf{R}_x \mathbf{B}^H) & \text{tr}(\mathbf{B} \mathbf{R}_x \mathbf{B}^H) \end{bmatrix} \succeq \mathbf{0}. \quad (15)$$

Accordingly, problem (P2.1) is equivalent to the following semi-definite program (SDP), which can be optimally solved by convex solvers such as CVX [18]:

$$(P2.2) : \max_{\mathbf{R}_x, t} t$$

s.t. (13a), (13b), and (15).

### B. Reflective Beamforming Optimization

Next, we optimize the reflecting beamformer  $\mathbf{v}$  in problem (P1) under any given transmit beamformer  $\mathbf{R}_x$ , in which the CRLB formula in (11) is used. In this case, the reflective beamforming optimization problem is formulated as

$$(P3) : \max_{\mathbf{v}} \left( \mathbf{v}^H \mathbf{R}_2 \mathbf{v} \left( \mathbf{v}^H \mathbf{D} \mathbf{R}_1 \mathbf{D} \mathbf{v} - \frac{|\mathbf{v}^H \mathbf{D} \mathbf{R}_1 \mathbf{v}|^2}{\mathbf{v}^H \mathbf{R}_1 \mathbf{v}} \right) + \mathbf{v}^H \mathbf{R}_1 \mathbf{v} \left( \mathbf{v}^H \mathbf{D} \mathbf{R}_2 \mathbf{D} \mathbf{v} - \frac{|\mathbf{v}^H \mathbf{D} \mathbf{R}_2 \mathbf{v}|^2}{\mathbf{v}^H \mathbf{R}_2 \mathbf{v}} \right) \right)$$

s.t. (13d),

which is still non-convex due to the non-concavity of the objective function and the unit-modulus constraint in (13d). To resolve this issue, in the following we first deal with constraint (13d) based on the idea of SDR, and then use SCA to approximate the relaxed problem as convex ones.

First, we use the idea of SDR to deal with the unit-modulus constraint in (13d). We define  $\mathbf{V} = \mathbf{v} \mathbf{v}^H$  with  $\mathbf{V} \succeq \mathbf{0}$  and  $\text{rank}(\mathbf{V}) = 1$ . As a result, it follows based on (13d) that  $\mathbf{V}_{n,n} = 1, \forall n \in \{1, 2, \dots, N\}$ . Also, we have  $\mathbf{v}^H \mathbf{R}_1 \mathbf{v} = \text{tr}(\mathbf{R}_1 \mathbf{V})$ ,  $\mathbf{v}^H \mathbf{R}_2 \mathbf{v} = \text{tr}(\mathbf{R}_2 \mathbf{V})$ ,  $\mathbf{v}^H \mathbf{D} \mathbf{R}_1 \mathbf{v} = \text{tr}(\mathbf{D} \mathbf{R}_1 \mathbf{V})$ ,  $\mathbf{v}^H \mathbf{D} \mathbf{R}_2 \mathbf{v} = \text{tr}(\mathbf{D} \mathbf{R}_2 \mathbf{V})$ ,  $\mathbf{v}^H \mathbf{D} \mathbf{R}_1 \mathbf{D} \mathbf{v} = \text{tr}(\mathbf{D} \mathbf{R}_1 \mathbf{D} \mathbf{V})$ , and  $\mathbf{v}^H \mathbf{D} \mathbf{R}_2 \mathbf{D} \mathbf{v} = \text{tr}(\mathbf{D} \mathbf{R}_2 \mathbf{D} \mathbf{V})$ . By substituting  $\mathbf{V} = \mathbf{v} \mathbf{v}^H$  and introducing two auxiliary variables  $t_1$  and  $t_2$ , problem (P3) is equivalently re-expressed as

$$(P3.1) : \max_{\mathbf{V}, t_1, t_2} f_1(\mathbf{V}, t_1, t_2) + f_2(\mathbf{V}, t_1, t_2)$$

s.t.  $\mathbf{V}_{n,n} = 1, \forall n \in \{1, 2, \dots, N\}$  (16a)

$\mathbf{V} \succeq \mathbf{0}$  (16b)

$\text{rank}(\mathbf{V}) = 1$  (16c)

$t_1 \geq \frac{|\text{tr}(\mathbf{D} \mathbf{R}_1 \mathbf{V})|^2}{\text{tr}(\mathbf{R}_1 \mathbf{V})}$  (16d)

$t_2 \geq \frac{|\text{tr}(\mathbf{D} \mathbf{R}_2 \mathbf{V})|^2}{\text{tr}(\mathbf{R}_2 \mathbf{V})}$ , (16e)

where

$$\begin{aligned} f_1(\mathbf{V}, t_1, t_2) &= \frac{1}{4} \text{tr}^2((\mathbf{R}_2 + \mathbf{D} \mathbf{R}_1 \mathbf{D}) \mathbf{V}) + \frac{1}{4} (\text{tr}(\mathbf{R}_2 \mathbf{V} - t_1)^2 \\ &\quad + \frac{1}{4} \text{tr}^2((\mathbf{R}_1 + \mathbf{D} \mathbf{R}_2 \mathbf{D}) \mathbf{V}) + \frac{1}{4} (\text{tr}(\mathbf{R}_1 \mathbf{V} - t_2)^2) \end{aligned}$$

and

$$\begin{aligned} f_2(\mathbf{V}, t_1, t_2) &= -\frac{1}{4} \text{tr}^2((\mathbf{R}_2 - \mathbf{D} \mathbf{R}_1 \mathbf{D}) \mathbf{V}) - \frac{1}{4} (\text{tr}(\mathbf{R}_2 \mathbf{V} + t_1)^2 \\ &\quad - \frac{1}{4} \text{tr}^2((\mathbf{R}_1 - \mathbf{D} \mathbf{R}_2 \mathbf{D}) \mathbf{V}) - \frac{1}{4} (\text{tr}(\mathbf{R}_1 \mathbf{V} + t_2)^2). \end{aligned}$$

Here,  $f_1(\mathbf{V}, t_1, t_2)$  and  $f_2(\mathbf{V}, t_1, t_2)$  are convex and concave functions, respectively. Using the Schur complement [17], the constraints in (16d) and (16e) are equivalently transformed into the following convex semi-definite constraints:

$$\begin{bmatrix} t_1 & \text{tr}(\mathbf{D} \mathbf{R}_1 \mathbf{V}) \\ \text{tr}(\mathbf{V}^H \mathbf{R}_1^H \mathbf{D}^H) & \text{tr}(\mathbf{R}_1 \mathbf{V}) \end{bmatrix} \succeq \mathbf{0}, \quad (17)$$

$$\begin{bmatrix} t_2 & \text{tr}(\mathbf{D} \mathbf{R}_2 \mathbf{V}) \\ \text{tr}(\mathbf{V}^H \mathbf{R}_2^H \mathbf{D}^H) & \text{tr}(\mathbf{R}_2 \mathbf{V}) \end{bmatrix} \succeq \mathbf{0}. \quad (18)$$

Problem (P3.1) is then equivalent to the following problem:

$$(P3.2) : \max_{\mathbf{V}, t_1, t_2} f_1(\mathbf{V}, t_1, t_2) + f_2(\mathbf{V}, t_1, t_2)$$

s.t. (16a), (16b), (16c), (17), and (18).

By dropping the rank-one constraint in (16c), we get the relaxed version of problem (P3.2) without constraint (16c), denoted by problem (P3.3):

$$(P3.3) : \max_{\mathbf{V}, t_1, t_2} f_1(\mathbf{V}, t_1, t_2) + f_2(\mathbf{V}, t_1, t_2)$$

s.t. (16a), (16b), (17), and (18).

Note that in problem (P3.3), all constraints are convex and only  $f_1(\mathbf{V}, t_1, t_2)$  in the objective function is non-concave.

Then, we use SCA to solve the non-convex problem (P3.3), which approximates it as a series of convex problems. The SCA-based solution to problem (P3.3) is implemented in an iterative manner as follows. Consider each iteration  $r \geq 1$ , in which the local point is denoted by  $\mathbf{V}^{(r)}$ ,  $t_1^{(r)}$ , and  $t_2^{(r)}$ . Then based on the local point, we obtain a global linear lower bound function  $\hat{f}_1^{(r)}(\mathbf{V}, t_1, t_2)$  for the convex function  $f_1(\mathbf{V}, t_1, t_2)$  in problem (P3.3), based on its first-order Taylor expansion, i.e.,

$$\begin{aligned} &f_1(\mathbf{V}, t_1, t_2) \\ &\geq f_1(\mathbf{V}^{(r)}, t_1^{(r)}, t_2^{(r)}) + \frac{1}{2} \text{tr}((\mathbf{R}_2 + \mathbf{D} \mathbf{R}_1 \mathbf{D}) \mathbf{V}^{(r)}) \\ &\quad \text{tr}((\mathbf{R}_2 + \mathbf{D} \mathbf{R}_1 \mathbf{D})(\mathbf{V} - \mathbf{V}^{(r)})) + \frac{1}{2} \text{tr}((\mathbf{R}_1 \\ &\quad + \mathbf{D} \mathbf{R}_2 \mathbf{D}) \mathbf{V}^{(r)}) \text{tr}((\mathbf{R}_1 + \mathbf{D} \mathbf{R}_2 \mathbf{D})(\mathbf{V} - \mathbf{V}^{(r)})) \\ &\quad + \frac{1}{2} t_1^{(r)}(t_1 - t_1^{(r)}) + \frac{1}{2} t_2^{(r)}(t_2 - t_2^{(r)}) \\ &\quad + \frac{1}{2} \text{tr}(\mathbf{R}_2 \mathbf{V}^{(r)}) \text{tr}(\mathbf{R}_2(\mathbf{V} - \mathbf{V}^{(r)})) \\ &\quad + \frac{1}{2} \text{tr}(\mathbf{R}_1 \mathbf{V}^{(r)}) \text{tr}(\mathbf{R}_1(\mathbf{V} - \mathbf{V}^{(r)})) \\ &\triangleq \hat{f}_1^{(r)}(\mathbf{V}, t_1, t_2). \end{aligned}$$

By replacing  $f_1(\mathbf{V}, t_1, t_2)$  as  $\hat{f}_1^{(r)}(\mathbf{V}, t_1, t_2)$ , problem (P3.3) is approximated as the following convex form

$$(P3.3) : \max_{\mathbf{V}, t_1, t_2} \hat{f}_1^{(r)}(\mathbf{V}, t_1, t_2) + f_2(\mathbf{V}, t_1, t_2)$$

s.t. (16a), (16b), (17), and (18),

which can be optimally solved by convex solvers such as CVX [18]. Let  $\tilde{\mathbf{V}}^*$ ,  $\tilde{t}_1^*$ , and  $\tilde{t}_2^*$  denote the optimal solution to problem (P3.3), which is then updated to be the local point  $\mathbf{V}^{(r+1)}$ ,  $t_1^{(r+1)}$ , and  $t_2^{(r+1)}$  for the next iteration. Note that as  $\hat{f}_1^{(r)}(\mathbf{V}, t_1, t_2)$  serves as a lower bound of  $f_1(\mathbf{V}, t_1, t_2)$ , it is ensured that  $f_1(\mathbf{V}^{(r+1)}, t_1^{(r+1)}, t_2^{(r+1)}) + f_2(\mathbf{V}^{(r+1)}, t_1^{(r+1)}, t_2^{(r+1)}) \geq f_1(\mathbf{V}^{(r)}, t_1^{(r)}, t_2^{(r)}) + f_2(\mathbf{V}^{(r)}, t_1^{(r)}, t_2^{(r)})$ , i.e., the iteration leads to a non-decreasing objective value for problem (P3.3). Therefore, the convergence of SCA for solving problem (P3.3) is ensured. Let  $\tilde{\mathbf{V}}$ ,  $\tilde{t}_1$ , and  $\tilde{t}_2$  denote the obtained solution to problem (P3.3) based on SCA, where  $\text{rank}(\tilde{\mathbf{V}}) > 1$  may hold in general.

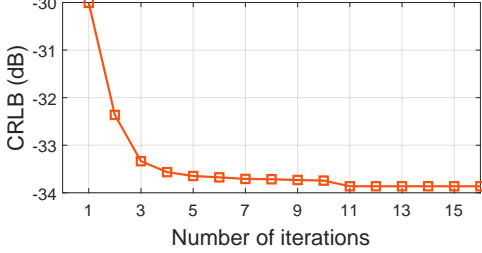


Figure 2. Convergence behavior of the proposed alternating optimization based algorithm for solving problem (P1), where  $P_0 = 40$  dBm.

Finally, we need to construct an approximate rank-one solution of  $\mathbf{V}$  to problem (P3.2) or (P3). We use the Gaussian randomization to resolve this issue. Specifically, we first generate a number of random realizations  $\mathbf{z} \sim \mathcal{CN}(\mathbf{0}, \tilde{\mathbf{V}})$ , and accordingly construct a set of candidate feasible solutions as  $\mathbf{v} = e^{j\arg(\mathbf{z})}$ . We then choose the best  $\mathbf{v}$  that achieves the maximum objective value of problem (P3.2) or (P3). Note that the Gaussian randomization should be implemented sufficiently many times to ensure that the objective value increases at each iteration of alternating optimization.

### C. Complete Algorithm of Alternating Optimization

Based on the results in Sections IV-A and IV-B, the alternating optimization based algorithm for solving problem (P1) is complete. In each iteration, we first solve problem (P2) to update the transmit beamformer  $\mathbf{R}_x$  with the updated reflective beamformer  $\mathbf{v}$  in the previous round, and then solve problem (P3) to update  $\mathbf{v}$  with the updated  $\mathbf{R}_x$ . Note that in each iteration of alternating optimization, problem (P2) is optimally solved, thus leading to a non-increasing CRLB value. Also notice that with sufficient number of Gaussian randomizations, the obtained solution to problem (P3) is also ensured to result in a monotonically non-increasing CRLB. As a result, the convergence of the proposed alternating optimization based algorithm for solving problem (P1) is ensured.

## V. NUMERICAL RESULTS

This section provides numerical results to evaluate the performance of our proposed joint beamforming design based on CRLB minimization. We consider the Rician fading channel for the AP-IRS link with the Rician factor being 0.5. We consider the distance-dependent path loss  $K_0(\frac{d}{d_0})^{-\alpha_0}$ , where  $d$  is the distance of the transmission link and  $K_0 = -30$  dB is the path loss at the reference distance  $d_0 = 1$  m, and the path-loss exponent  $\alpha_0$  is set as 2.5 for the AP-IRS and IRS-target links. The AP, target, and IRS are located at coordinate  $(0, 0)$ ,  $(12$  m,  $0)$ , and  $(3$  m,  $3$  m), respectively. We set the number of antennas at the AP, the number of reflecting elements at the IRS, and the radar dwell time slots as  $M = 8$ ,  $N = 8$ , and  $T = 256$ , respectively. We also set the target's RCS as one and the noise power at the AP as  $\sigma^2 = -120$  dBm, respectively.

Fig. 2 shows the convergence behavior of our proposed alternating optimization based algorithm for solving problem (P1), where  $P_0 = 40$  dBm. It is shown that the proposed

alternating optimization based algorithm converges within around 11 iterations, thus validating its effectiveness.

Next, we evaluate the estimation performance of our proposed joint beamforming design based on CRLB minimization for IRS-enabled sensing as compared to the following benchmark schemes.

1) *SNR maximization*: We maximize the received SNR of the echo signal at the AP in (2), by jointly optimizing the transmit beamforming at the AP and reflective beamforming at the IRS. First, by applying maximum-ratio combining at the receiver of the AP, the average SNR of the echo signals is

$$\begin{aligned}\gamma &= \frac{1}{T} \sum_{t=1}^T \frac{\|\mathbf{y}(t)\|^2}{\sigma^2} \\ &= \frac{|\alpha|^2 \|\mathbf{G}^T \mathbf{A} \mathbf{v}\|^2}{\sigma^2} \text{tr}((\mathbf{G}^T \mathbf{A} \mathbf{v})^* (\mathbf{G}^T \mathbf{A} \mathbf{v})^T \mathbf{R}_x).\end{aligned}\quad (19)$$

Then, for any given reflective beamformer  $\mathbf{v}$ , it is known that maximum-ratio transmission is the optimal transmit beamforming solution, i.e.,

$$\hat{\mathbf{R}}_x = \frac{P_0 \mathbf{G}^H \mathbf{A}^* \mathbf{v}^* \mathbf{v}^T \mathbf{A}^T \mathbf{G}}{\|\mathbf{G}^T \mathbf{A} \mathbf{v}\|^2}. \quad (20)$$

Next, by substituting  $\hat{\mathbf{R}}_x$  in (20) back into (19), we have

$$\gamma = \frac{P_0 |\alpha|^2}{\sigma^2} \|\mathbf{G}^T \mathbf{A} \mathbf{v}\|^4. \quad (21)$$

Finally, the reflective beamforming  $\mathbf{v}$  at the IRS is optimized to maximize  $\|\mathbf{G}^T \mathbf{A} \mathbf{v}\|^2$ , subject to the unit-modulus constraint in (13d), which is similar to the SNR maximization in IRS-enabled multiple-input single-output (MISO) communications that has been studied in [4].

2) *Reflective beamforming only with isotropic transmission (Reflective BF only)*: The AP uses the isotropic transmission by transmitting orthonormal signal beams and setting  $\mathbf{R}_x = P_0 / M \mathbf{I}_M$ . Then, the reflective beamforming at the IRS is optimized to minimize the CRLB by solving problem (P3).

3) *Transmit beamforming only with random phase shifts (Transmit BF only)*: We consider the random reflecting phase shifts at the IRS, based on which the transmit beamforming at the AP is optimized to minimize the CRLB by solving problem (P2).

Furthermore, note that besides the CRLB, we also implement the practical MLE method to estimate the target's DoA  $\theta$ , and accordingly evaluate the estimation MSE as the performance metric for gaining more insights. For brevity, please refer to Appendix C for the details of MLE for DoA estimation.

Fig. 3 shows the CRLB and the estimation MSE with MLE versus the transmit power budget  $P$  at the AP. It is observed that the derived CRLB is identical to the estimation MSE with MLE at the high SNR regime. This is consistent with the results in [12] and validates the CRLB derivation. It is also observed that the proposed CRLB minimization scheme achieves the lowest CRLB in the whole transmit power regime, which shows the effectiveness of our proposed joint beamforming design in CRLB minimization. Furthermore, when the transmit power is sufficiently high (e.g.,  $P_0 > 36$  dBm), the

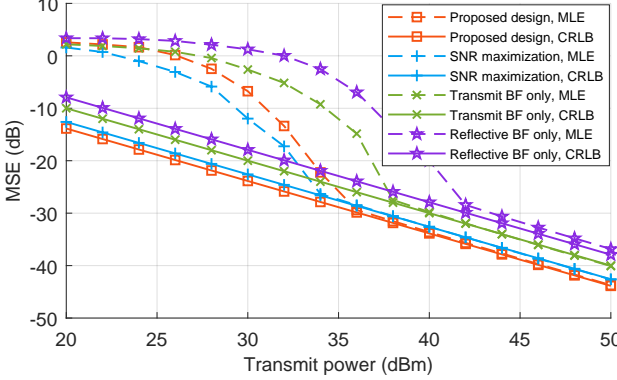


Figure 3. The MSE performance for target estimation versus the transmit power budget  $P$  at the AP.

proposed CRLB minimization scheme is observed to achieve lower estimation MSE than the three benchmark schemes. When the transmit power is low (e.g.,  $P_0 < 36$  dBm), the SNR maximization scheme is observed to achieve lower estimation MSE (under MLE) than the proposed CRLB minimization scheme. This is because that in this case, the CRLB is not achievable using MLE, and the estimation performance of MLE is particularly sensitive to the power of echo signals, thus making the SNR maximization scheme desirable.

## VI. CONCLUSION

This work considered an IRS-enabled NLoS wireless sensing system consisting of an AP with multiple antennas, an ULA-IRS with multiple reflecting elements, and a target at the NLoS region of the AP. The AP aimed to estimate the target's DoA w.r.t. the IRS based on the echo signal received at the AP from the AP-IRS-target-IRS-AP link. Under this setup, we jointly design the transmit beamforming at the AP and the reflective beamforming at the IRS to minimize the DoA estimation error in terms of CRLB. Towards this end, we obtained the CRLB for DoA estimation in closed form and then minimized the obtained CRLB by jointly optimizing the transmit and reflective beamforming. Numerical results showed that the proposed algorithm achieved improved estimation performance in terms of estimation MSE, especially when the SNR became large. We envision that this work can provide new insights in designing IRS-enabled sensing and IRS-enabled ISAC systems.

## APPENDIX A THE DERIVATION OF THE FIM IN (6)

As the covariance matrix  $\mathbf{R}_n$  of noise  $\tilde{\mathbf{n}}$  is independent with  $\xi$ , we have  $\frac{\partial \mathbf{R}_n}{\partial \xi_i} = 0, i = 1, 2, 3$ , in (5). Furthermore, we have

$$\frac{\partial \tilde{\mathbf{u}}}{\partial \theta} = \text{a} \text{vec}(\dot{\mathbf{B}}\mathbf{X}), \quad (22)$$

$$\frac{\partial \tilde{\mathbf{u}}}{\partial \tilde{\alpha}} = [1, j] \otimes \text{vec}(\mathbf{B}\mathbf{X}). \quad (23)$$

Accordingly, it follows that

$$\begin{aligned} \mathbf{F}_{\theta\theta} &= \frac{2}{\sigma^2} \text{Re}\{(\text{a} \text{vec}(\dot{\mathbf{B}}\mathbf{X}))^H \text{a} \text{vec}(\dot{\mathbf{B}}\mathbf{X})\} \\ &= \frac{2|\alpha|^2}{\sigma^2} \text{Re}\{\text{tr}(\dot{\mathbf{B}}\mathbf{X})^H (\dot{\mathbf{B}}\mathbf{X})\} \\ &= \frac{2|\alpha|^2}{\sigma^2} \text{Re}\{\text{tr}(\dot{\mathbf{B}}\mathbf{X}\mathbf{X}^H \dot{\mathbf{B}}^H)\} \\ &= \frac{2T|\alpha|^2}{\sigma^2} \text{tr}(\dot{\mathbf{B}}\mathbf{R}_x \dot{\mathbf{B}}^H), \end{aligned} \quad (24)$$

$$\begin{aligned} \mathbf{F}_{\theta\tilde{\alpha}} &= \frac{2}{\sigma^2} \text{Re}\{(\text{a} \text{vec}(\dot{\mathbf{B}}\mathbf{X}))^H [1, j] \otimes \text{vec}(\mathbf{B}\mathbf{X})\} \\ &= \frac{2}{\sigma^2} \text{Re}\{\alpha^*[1, j] \otimes (\text{vec}(\dot{\mathbf{B}}\mathbf{X})^H \text{vec}(\mathbf{B}\mathbf{X}))\} \\ &= \frac{2}{\sigma^2} \text{Re}\{\alpha^*[1, j] (\text{tr}(\dot{\mathbf{B}}\mathbf{X})^H \mathbf{B}\mathbf{X})\} \\ &= \frac{2T}{\sigma^2} \text{Re}\{\alpha^* \text{tr}(\mathbf{B}\mathbf{R}_x \dot{\mathbf{B}}^H)[1, j]\}, \end{aligned} \quad (25)$$

$$\begin{aligned} \mathbf{F}_{\tilde{\alpha}\tilde{\alpha}} &= \frac{2}{\sigma^2} \text{Re}\{([1, j] \otimes \text{vec}(\mathbf{B}\mathbf{X}))^H ([1, j] \otimes \text{vec}(\mathbf{B}\mathbf{X}))\} \\ &= \frac{2}{\sigma^2} \text{Re}\{[1, j]^H \otimes [1, j] \text{vec}(\mathbf{B}\mathbf{X})^H \text{vec}(\mathbf{B}\mathbf{X})\} \\ &= \frac{2}{\sigma^2} \text{Re}\{\mathbf{I}_2 \text{tr}((\mathbf{B}\mathbf{X})^H \mathbf{B}\mathbf{X})\} \\ &= \frac{2T}{\sigma^2} \text{tr}(\mathbf{B}\mathbf{R}_x \mathbf{B}^H) \mathbf{I}_2. \end{aligned} \quad (26)$$

Therefore, the FIM in (6) is obtained.

## APPENDIX B PROOF OF PROPOSITION 1

Note that the determinant of the FIM  $\mathbf{F}$  is

$$\begin{aligned} &\det(\mathbf{F}) \\ &= \frac{8T^3|\alpha|^2}{\sigma^6} \left( \text{tr}(\mathbf{B}\mathbf{R}_x \mathbf{B}^H) \text{tr}(\dot{\mathbf{B}}\mathbf{R}_x \dot{\mathbf{B}}^H) \right. \\ &\quad \left. - |\text{tr}(\mathbf{B}\mathbf{R}_x \dot{\mathbf{B}}^H)|^2 \right) \\ &= \frac{8T^3|\alpha|^2}{\sigma^6} \left( \|(\mathbf{W}\Lambda^{1/2})^T \mathbf{b}\|^4 (\|\dot{\mathbf{b}}\|^2 \|\mathbf{b}\|^2 - |\dot{\mathbf{b}}^H \mathbf{b}|^2) \right. \\ &\quad \left. + \|\mathbf{b}\|^4 (\|(\mathbf{W}\Lambda^{1/2})^T \dot{\mathbf{b}}\|^2 \|(\mathbf{W}\Lambda^{1/2})^T \mathbf{b}\|^2 \right. \\ &\quad \left. - |\dot{\mathbf{b}}^H (\mathbf{W}\Lambda^{1/2})^* (\mathbf{W}\Lambda^{1/2})^T \mathbf{b}|^2) \right). \end{aligned} \quad (27)$$

First, suppose that  $\text{rank}(\mathbf{G}) = 1$ , for which we have the truncated SVD of  $\mathbf{G}$  as  $\mathbf{G} = \sigma_1 \hat{\mathbf{u}}_1 \hat{\mathbf{v}}_1^T$ , where  $\hat{\mathbf{u}}_1$  and  $\hat{\mathbf{v}}_1$  are the left and right dominant singular vectors, and  $\sigma_1$  denotes the dominant singular value. In this case, it follows that

$$\mathbf{b} = \sigma_1 \hat{\mathbf{v}}_1 \hat{\mathbf{u}}_1^T \mathbf{A} \mathbf{v}, \quad (28)$$

$$\dot{\mathbf{b}} = j\pi \cos \theta \sigma_1 \hat{\mathbf{v}}_1 \hat{\mathbf{u}}_1^T \mathbf{A} \mathbf{D} \mathbf{v}, \quad (29)$$

$$(\mathbf{W}\Lambda^{1/2})^T \mathbf{b} = (\mathbf{W}\Lambda^{1/2})^T \sigma_1 \hat{\mathbf{v}}_1 \hat{\mathbf{u}}_1^T \mathbf{A} \mathbf{v}, \quad (30)$$

$$(\mathbf{W}\Lambda^{1/2})^T \dot{\mathbf{b}} = (\mathbf{W}\Lambda^{1/2})^T j\pi \cos \theta \sigma_1 \hat{\mathbf{v}}_1 \hat{\mathbf{u}}_1^T \mathbf{A} \mathbf{D} \mathbf{v}. \quad (31)$$

It is clear that  $\dot{\mathbf{b}}$  and  $\mathbf{b}$  are aligned with each other, i.e.,

$$\dot{\mathbf{b}} = \frac{j\pi \cos \theta \hat{\mathbf{u}}_1^T \mathbf{A} \mathbf{D} \mathbf{v}}{\hat{\mathbf{u}}_1^T \mathbf{A} \mathbf{v}} \mathbf{b}, \quad (32)$$

such that

$$|\dot{\mathbf{b}}^H \mathbf{b}|^2 = \|\dot{\mathbf{b}}\|^2 \|\mathbf{b}\|^2. \quad (33)$$

Similarly, as  $(\mathbf{W}\Lambda^{1/2})^T \dot{\mathbf{b}}$  and  $(\mathbf{W}\Lambda^{1/2})^T \mathbf{b}$  are aligned with each other, we have

$$\begin{aligned} & |\dot{\mathbf{b}}^H (\mathbf{W}\Lambda^{1/2})^* (\mathbf{W}\Lambda^{1/2})^T \dot{\mathbf{b}}|^2 \\ & = \|(\mathbf{W}\Lambda^{1/2})^T \dot{\mathbf{b}}\|^2 \|(\mathbf{W}\Lambda^{1/2})^T \mathbf{b}\|^2. \end{aligned} \quad (34)$$

As a result, we have  $\det(\mathbf{F}) = 0$ , which implies that the FIM  $\mathbf{F}$  is not invertible. Accordingly, the CRLB for DoA estimation is unbounded.

Next, suppose that  $\text{rank}(\mathbf{G}) > 1$ , in this case  $\dot{\mathbf{b}}$  and  $\mathbf{b}$  are not aligned with each other. According to the Cauchy-Schwarz inequality, we have

$$|\dot{\mathbf{b}}^H \mathbf{b}|^2 < \|\dot{\mathbf{b}}\|^2 \|\mathbf{b}\|^2. \quad (35)$$

Similarly, as  $(\mathbf{W}\Lambda^{1/2})^T \dot{\mathbf{b}}$  and  $(\mathbf{W}\Lambda^{1/2})^T \mathbf{b}$  are not aligned with each other, we have

$$\begin{aligned} & |\dot{\mathbf{b}}^H (\mathbf{W}\Lambda^{1/2})^* (\mathbf{W}\Lambda^{1/2})^T \dot{\mathbf{b}}|^2 \\ & < \|(\mathbf{W}\Lambda^{1/2})^T \dot{\mathbf{b}}\|^2 \|(\mathbf{W}\Lambda^{1/2})^T \mathbf{b}\|^2. \end{aligned} \quad (36)$$

In this case, the FIM  $\mathbf{F}$  is invertible, such that the CRLB is bounded. Proposition 1 is proved.

## APPENDIX C MLE FOR ESTIMATING TARGET'S DOA

Based on (4), the vectorized received signal at the AP is rewritten as

$$\tilde{\mathbf{y}} = \alpha \mathbf{d}(\theta) + \tilde{\mathbf{n}}, \quad (37)$$

where  $\mathbf{d}(\theta) = \text{vec}(\mathbf{B}\mathbf{X})$ . The likelihood function of  $\tilde{\mathbf{y}}$  given  $\xi$  is

$$f_{\tilde{\mathbf{y}}}(\tilde{\mathbf{y}}; \xi) = \frac{1}{(\pi\sigma^2)^{MT}} \exp\left(-\frac{1}{\sigma^2} \|\tilde{\mathbf{y}} - \alpha \mathbf{d}(\theta)\|^2\right). \quad (38)$$

In this case, maximizing  $f_{\tilde{\mathbf{y}}}(\tilde{\mathbf{y}}; \xi)$  is equivalent to minimizing  $\|\tilde{\mathbf{y}} - \alpha \mathbf{d}(\theta)\|^2$ . Hence, the MLE of  $\theta$  and  $\alpha$  is given by

$$(\hat{\theta}_{\text{MLE}}, \hat{\alpha}_{\text{MLE}}) = \arg \min_{\theta, \alpha} \|\tilde{\mathbf{y}} - \alpha \mathbf{d}(\theta)\|^2. \quad (39)$$

Note that under any given  $\theta$ , the MLE of  $\alpha$  is obtained as

$$\hat{\alpha}_{\text{MLE}} = (\mathbf{d}^H(\theta) \mathbf{d}(\theta))^{-1} \mathbf{d}^H(\theta) \tilde{\mathbf{y}} = \frac{\mathbf{d}^H(\theta) \tilde{\mathbf{y}}}{\|\mathbf{d}(\theta)\|^2}. \quad (40)$$

By substituting (40) back into (39), we have

$$\begin{aligned} \|\tilde{\mathbf{y}} - \hat{\alpha}_{\text{MLE}} \mathbf{d}(\theta)\|^2 & = \|\tilde{\mathbf{y}}\|^2 - \frac{|\mathbf{d}^H(\theta) \tilde{\mathbf{y}}|^2}{\|\mathbf{d}(\theta)\|^2} \\ & = \|\text{vec}(\mathbf{Y})\|^2 - \frac{|\text{vec}(\mathbf{B}\mathbf{X})^H \text{vec}(\mathbf{Y})|^2}{\|\text{vec}(\mathbf{B}\mathbf{X})^H \text{vec}(\mathbf{B}\mathbf{X})\|^2} \\ & = \|\text{vec}(\mathbf{Y})\|^2 - \frac{|\text{tr}(\mathbf{B}^H \mathbf{Y} \mathbf{X}^H)|^2}{\|\mathbf{B}^H \mathbf{Y} \mathbf{X}^H\|^2} \\ & = \|\text{vec}(\mathbf{Y})\|^2 - \frac{|\mathbf{b}^H \mathbf{Y} \mathbf{X}^H \mathbf{b}^*|^2}{T \text{tr}(\mathbf{B}^H \mathbf{R}_x^H \mathbf{B}^H)} \\ & = \|\text{vec}(\mathbf{Y})\|^2 - \frac{|\mathbf{b}^H \mathbf{Y} \mathbf{X}^H \mathbf{b}^*|^2}{T \|\mathbf{b}\|^2 \mathbf{b}^H \mathbf{R}_x^H \mathbf{b}}. \end{aligned} \quad (41)$$

As a result, by substituting (41) into (39), the MLE of  $\theta$  becomes

$$\hat{\theta}_{\text{MLE}} = \arg \max_{\theta} \frac{|\mathbf{b}^H \mathbf{Y} \mathbf{X}^H \mathbf{b}^*|^2}{T \|\mathbf{b}\|^2 \mathbf{b}^H \mathbf{R}_x^H \mathbf{b}}, \quad (42)$$

which can be obtained via exhaustive search over  $[-\frac{\pi}{2}, \frac{\pi}{2}]$ .

## REFERENCES

- [1] X. Song, D. Zhao, H. Hua, T. X. Han, X. Yang, and J. Xu, "Joint transmit and reflective beamforming for IRS-assisted integrated sensing and communication," in *Proc. IEEE WCNC Workshop*, Austin, TX, USA, Apr. 2022.
- [2] F. Liu, C. Masouros, A. P. Petropulu, H. Griffiths, and L. Hanzo, "Joint radar and communication design: Applications, state-of-the-art, and the road ahead," *IEEE Trans. Commun.*, vol. 68, no. 6, pp. 3834–3862, Jun. 2020.
- [3] F. Liu, Y. Cui, C. Masouros, J. Xu, T. X. Han, Y. C. Eldar, and S. Buzzi, "Integrated sensing and communications: Towards dual-functional wireless networks for 6G and beyond," *IEEE J. Sel. Areas Commun.*, early access, 2022.
- [4] Q. Wu and R. Zhang, "Intelligent reflecting surface enhanced wireless network via joint active and passive beamforming," *IEEE Trans. Wireless Commun.*, vol. 18, no. 11, pp. 5394–5409, Nov. 2019.
- [5] Q. Wu, S. Zhang, B. Zheng, C. You, and R. Zhang, "Intelligent reflecting surface-aided wireless communications: A tutorial," *IEEE Trans. Commun.*, vol. 69, no. 5, pp. 3313–3351, May 2021.
- [6] S. Gong, X. Lu, D. T. Hoang, D. Niyato, L. Shu, D. I. Kim, and Y.-C. Liang, "Toward smart wireless communications via intelligent reflecting surfaces: A contemporary survey," *IEEE Commun. Surv. Tutor.*, vol. 22, no. 4, pp. 2283–2314, Jun. 2020.
- [7] A. Aubry, A. De Maio, and M. Rosamilia, "Reconfigurable intelligent surfaces for N-LOS radar surveillance," *IEEE Trans. Veh. Technol.*, vol. 70, no. 10, pp. 10735–10749, Oct. 2021.
- [8] X. Shao, C. You, W. Ma, X. Chen, and R. Zhang, "Target sensing with intelligent reflecting surface: Architecture and performance," *IEEE J. Sel. Areas Commun.*, early access, 2022.
- [9] W. Lu, Q. Lin, N. Song, Q. Fang, X. Hua, and B. Deng, "Target detection in intelligent reflecting surface aided distributed MIMO radar systems," *IEEE Sens. Lett.*, vol. 5, no. 3, pp. 1–4, Mar. 2021.
- [10] S. Buzzi, E. Grossi, M. Lops, and L. Venturino, "Foundations of MIMO radar detection aided by reconfigurable intelligent surfaces," *IEEE Trans. Signal Process.*, early access, 2022.
- [11] Z.-M. Jiang, M. Rihan, P. Zhang, L. Huang, Q. Deng, J. Zhang, and E. M. Mohamed, "Intelligent reflecting surface aided dual-function radar and communication system," *IEEE Syst. J.*, pp. 1–12, Feb. 2021.
- [12] S. M. Kay, *Fundamentals of Statistical Signal Processing: Estimation Theory*. Prentice-hall Englewood Cliffs, NJ, 1993, no. 493–563.
- [13] I. Bekkerman and J. Tabrikian, "Target detection and localization using MIMO radars and sonars," *IEEE Trans. Signal Process.*, vol. 54, no. 10, pp. 3873–3883, Oct. 2006.
- [14] F. Liu, Y.-F. Liu, A. Li, C. Masouros, and Y. C. Eldar, "Cramér-Rao bound optimization for joint radar-communication beamforming," *IEEE Trans. Signal Process.*, vol. 70, pp. 240–253, Dec. 2021.
- [15] H. Hua, J. Xu, and T. X. Han, "Optimal transmit beamforming for integrated sensing and communication," 2021. [Online]. Available: <https://arxiv.org/pdf/2104.11871.pdf>
- [16] B. Zheng, C. You, W. Mei, and R. Zhang, "A survey on channel estimation and practical passive beamforming design for intelligent reflecting surface aided wireless communications," *IEEE Commun. Surv. Tutor.*, pp. 1–1, Feb. 2022.
- [17] F. Zhang, *The Schur Complement and its Applications*. Springer Science & Business Media, 2006, vol. 4.
- [18] M. Grant and S. Boyd, "CVX: Matlab software for disciplined convex programming, version 2.1," <http://cvxr.com/cvx>, Mar. 2014.